Spectral Dependence of Light-induced Microwave Reflection Coefficient from Optoelectronic Waveguide Gratings

Walter Platte

Abstract—**After a short description of the method of operation of optoelectronic microwave filters, a detailed analysis of the spectral dependence of light-induced microwave reflection coefficient from an optoelectronically generated distributed Bragg reflection waveguide grating is reported. The theory is based on an improved stepped-impedance model utilizing a diffusion-controlled abrupt-profile approach of photoconductivity along with a conformal mapping technique for the quasi-static evaluation of the spectral performance of photoinduced wave attenuation. The validity of theory is clarified and the calculated results are compared with experimental results. As a useful result for future applications, an optimum excitation wavelength of about 825 nm for a fiber-optically controlled lab-tested 50Ω full-substrate silicon coplanar waveguide has been obtained.**

I. Introduction

THE DISTRIBUTED Bragg reflection (DBR) characteristics of a periodic-structure waveguide or transmission line can successfully be utilized for the realization of frequency-selective microwave or millimeter-wave devices such as band-reject filters [1] and grating reflectors, e.g., in a stabilized-feedback Gunn oscillator [2], [3]. Usually, the periodic perturbation in the direction of wave propagation is achieved by abrupt changes in permittivity or cross-sectional dimensions (e.g., reduced waveguide thickness [1]–[3]), thus producing a permanent, normally noncontrollable grating structure (Fig. 1(a)).

However, when replacing the total dielectric (or a suitable cross-sectional portion of it) by semiconductor material, it is possible to generate the grating configuration optoelectronically through an appropriate optical excitation of the semiconductor surface. For this purpose, the originally homogeneous, unperturbed semiconductor waveguide is photoexcited by a locally varying periodic CW illumination (Fig. 1(b)), which correspondingly causes a periodic distribution of the photoinduced charge carriers inside the semiconductor material. Thus, a nonpermanent photoconductivity grating is created.

Owing to constructive interference on the one hand and light-induced substrate losses on the other, a total light-induced microwave reflection coefficient of up to 40% (at X-band frequencies) can be achieved selectively. Since the grating period can be changed by altering the illumination pattern, such a finite periodically photoexcited transmission line structure may be developed for light-induced tunable filters or reflectors. Of course, its specific stopband behavior disappears at the light-off condition. In general, its microwave performance is governed by the inherent carrier diffusion mechanisms in such a way that the transverse diffusion mainly influences the light-induced losses [4], whereas the longitudinal carrier diffusion (in the direction of wave propagation) can effect a smooth

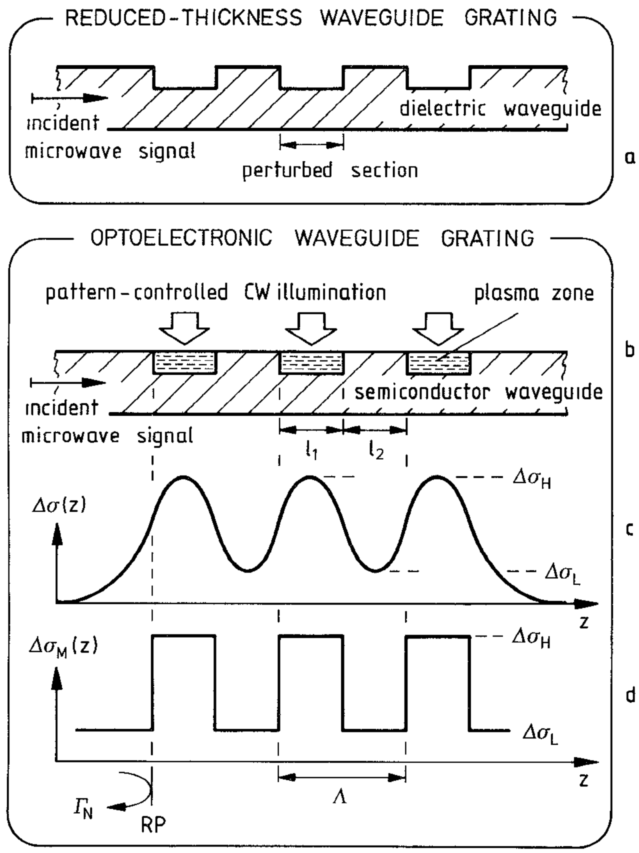

Fig. 1. (a) Longitudinal section of a square-shaped dielectric waveguide with permanent reduced-thickness DBR grating structure. (b) Longitudinal section of a square-shaped semiconductor waveguide with optically induced (nonpermanent) photoconductivity grating. (c) Actual distribution of photoconductivity $\Delta\sigma(z)$ in the case of substantial charge carrier diffusion into the (z-) direction of wave propagation. (d) Diffusion-controlled abrupt-profile approach of photoconductivity $\Delta\sigma_M(z)$, constituting the basis of the stepped-impedance model for the analysis of optoelectronic DBR gratings. For simplicity, a three-element grating structure ($N = 3$) with symmetric excitation ($l_1 = l_2$) is plotted. RP is the reference plane of total light-induced microwave reflection coefficient Γ_N.

Manuscript received January 15, 1993; revised March 24, 1994. This work was supported by the Gesellschaft der Freunde und Foerderer der Universitaet der Bundeswehr Hamburg e.V.

The author is with the Institut fuer Hochfrequenztechnik und Optoelektronik, Universitaet der Bundeswehr Hamburg, D-22043 Hamburg, Germany.

IEEE Log Number 9406815.

broadening of the grating profile (Fig. 1(c)), which reduces reflectance and selectivity [5], [6].

The total light-induced microwave reflection coefficient Γ_N from an N-element optoelectronic grating can be approximately calculated by means of an improved stepped-impedance model [7], which is based on the diffusion-controlled abrupt-profile approach of photoconductivity shown in Fig. 1(d). Herein, the high-level photoconductivity $\Delta\sigma_H$ of the excited section as well as the low-level photoconductivity $\Delta\sigma_L$ of the dark section is governed by longitudinal carrier diffusion. In comparison with the initial abrupt-profile concept used earlier [8] (where longitudinal carrier diffusion has been neglected), the introduction of a diffusion-controlled step height opens a more detailed and extensive DBR analysis (Section II).

Since the lengths l_1 and l_2 of the excited and dark sections, the period Λ (Fig. 1), the total length of the grating structure, and the amount of photoconductivity can be changed by altering the illumination pattern and the intensity, the grating parameters (i.e., center frequency, bandwidth, and reflectance) can be optically controlled. As an illustrative example, Fig. 2 shows the first lab-tested prototype of light-induced DBR microwave filter on silicon substrate illuminated by a pattern-controlled LED-fed fiber bundle array on top of the coplanar waveguide (CPW) [9]. The price one pays for the capability of optical control manifests itself in the optically induced losses that clearly injure the reflection and selectivity characteristics. However, it has been demonstrated from a numerical optimization of microwave performance with respect to the excitation pattern (with $l_1 \neq l_2$), the number of grating elements, and the controlling irradiance (at a given wavelength) that optimized optoelectronic waveguide gratings can exhibit DBR characteristics certainly comparable to those of dielectric permanent-grating devices [10].

Moreover, another improvement of DBR performance can be achieved by optimizing the optoelectronic parameters such as carrier lifetime τ, surface recombination velocity v_s, and optical wavelength λ. Concerning τ, an optimum value of about $10^{-5}s$ in bulk silicon was already derived and reported [5]. As to v_s, a perfect semiconductor surface with $v_s = 0$ would be best, but cannot be realized, of course. Hence, $v_s \leqq 2000$ cm/s should be considered to be the realistic optimum [11], which can be attained through the treatment of waver surface with special etchants or the evaporation of antirecombination coatings. Finally, as the absorption of light is a prerequisite of operation along with a dominant spectral dependence, λ can be also considered as a quantity that may be involved in the optimization procedure. For this reason, the spectral dependence of light-induced microwave reflection coefficient from a silicon CPW DBR grating is analyzed quantitatively in this paper, resulting in the optimum wavelength of optical excitation.

II. Light-Induced Microwave Reflection Coefficient

For the plasma-induced semiconductor CPW (Fig. 2) in which the major portion of losses is caused by the dominance of shunt conductance per unit length, the characteristic impedance Z_p may be approximately calculated from [5]

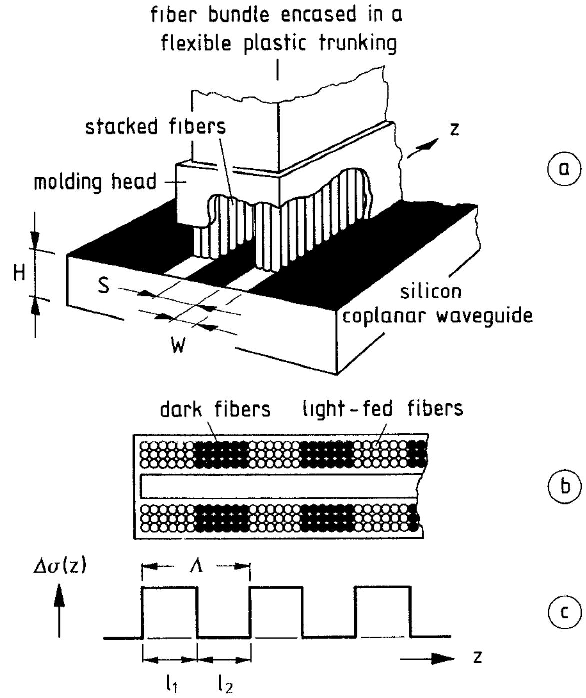

Fig. 2. Sketch of the first prototype of light-induced DBR microwave filter on silicon substrate illuminated by a pattern-controlled LED-fed fiber bundle array on top of the coplanar waveguide. (a) Total configuration with cutaway section of the molding head. (b) Cross-sectional view of the molding head. (c) Ideal profile of photoconductivity $\Delta\sigma(z)$ in the case of negligible longitudinal charge carrier diffusion.

$$Z_p \simeq Z_l(1 - j\Delta\vartheta_e)^{-1/2} \tag{1}$$

where Z_l is the real characteristic impedance of the dark CPW, e.g., $Z_l = 50\Omega$ [9], and $\Delta\vartheta_e$ is the effective photoconductivity loss tangent [5], [8]. Assuming uniform illumination in the direction of wave propagation (along with an inhomogeneous excitation in both transversal directions, of course), $\Delta\vartheta_e$ is given by [8]

$$\Delta\vartheta_e = (q_\epsilon q_p/\omega\epsilon_0\epsilon_{re})\Delta\sigma_e \tag{2}$$

where q_ϵ is the dielectric filling fraction [12], $\omega = 2\pi f$ with signal frequency f, ϵ_0 is the free space permittivity, and ϵ_{re} is the overall effective dielectric constant of the silicon CPW, including the upper half-space dielectric loading by the light-emitting stacked-fiber region of the molding head (Fig. 2) [9]. The plasma filling fraction q_p (which is identical to the term s/K used in [4]) takes account of the fact that only a fraction of the total CPW cross-section is really photoconductive. $\Delta\sigma_e$ is the effective CW-induced photoconductivity, which considers the actually inhomogeneous cross-sectional distribution of excess carrier density due to transversal carrier diffusion [4] (Section III).

When applying a locally periodic CW excitation in the direction of wave propagation, the induced photoconductivity $\Delta\sigma(z)$ also varies periodically exhibiting, in general, a smeared profile (Fig. 1(c)) caused by longitudinal carrier diffusion [13]. Referring to detailed investigations on the effect of profile broadening [7], the diffusion-controlled extreme

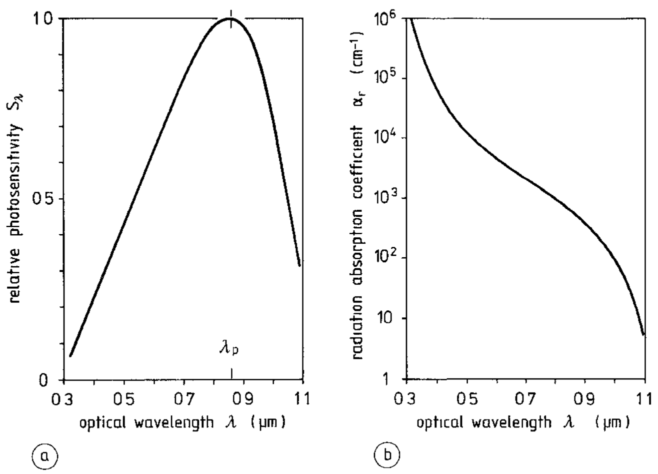

Fig. 3. (a) Relative spectral response S_λ (photosensitivity) of bulk silicon material at $T = 300$K exhibiting the peak wavelength $\lambda_p = 860$ nm. (b) Radiation absorption coefficient α_r of high-purity single-crystal silicon at $T = 300$K as a function of optical wavelength λ.

values $\Delta\sigma_H$ and $\Delta\sigma_L$ can be obtained from

$$\Delta\sigma_H \simeq \Delta\sigma_e[1 - \exp(-l_1/2L_a)] \tag{3a}$$

$$\Delta\sigma_L \simeq \Delta\sigma_e \exp(-l_1/2L_a) \tag{3b}$$

where L_a is the ambipolar diffusion length (Section III). Fig. (3a) and (3b) is valid for the number of grating elements $N \geqq 2$, symmetric excitation with $l_1 = l_2$, and $l_1/L_a \geqq 4$. Likewise, $\Delta\vartheta(z)$ varies periodically where the extreme values $\Delta\vartheta_H$, and $\Delta\vartheta_L$ may be obtained from (2) by replacing $\Delta\sigma_e$ with $\Delta\sigma_H$ or $\Delta\sigma_L$ from (3). Finally, when substituting $\Delta\vartheta_e$ by $\Delta\vartheta(z)$, it is seen from (1) that Z_p also shows a locally (and continuously) periodic variation. The resultant light-induced reflection coefficient Γ_N then can be exactly calculated by means of an appropriate integration procedure [14] which, in this case however, would imply an immense numerical effort. Therefore, an approximate calculation of Γ_N by means of a diffusion-controlled abrupt-profile approach of photoconductivity $\Delta\sigma_M(z)$ (Fig. 1(d)) is preferred. From this, a stepped-impedance profile $Z_p(z)$ with $Z_H = Z_p(\Delta\sigma_H)$ and $Z_L = Z_p(\Delta\sigma_L)$ is obtained causing the step reflection coefficient Γ_{st} from a single discontinuity according to

$$\Gamma_{st} = \frac{Z_H - Z_L}{Z_H + Z_L} \simeq \frac{(1 - j\Delta\vartheta_L)^{1/2} - (1 - j\Delta\vartheta_H)^{1/2}}{(1 - j\Delta\vartheta_L)^{1/2} + (1 - j\Delta\vartheta_H)^{1/2}} \tag{4}$$

where the microwave signal is assumed to propagate from the low-photoconductivity section into the high-photoconductivity section.

In the case of low excitation with $\Delta\vartheta_{H,L} \ll 1$, (4) yields $|\Gamma_{st}| \ll 1$. This allows us, from small-reflection theory [14], to calculate the reflection coefficient Γ_{ss} from a single excited section ($N = 1$) by summing up only the first-order contributions according to

$$\Gamma_{ss} \simeq \Gamma_{st}\{1 - \exp[-2l_1(\alpha_H + j\beta_H)]\} \tag{5}$$

where α_H is the (uniform) attenuation constant of the high-photoconductivity section and β_H is the phase constant. Likewise, supposing $|\Gamma_{ss}| \ll 1$, the total light-induced microwave reflection coefficient Γ_N from an N-element optoelectronic grating with symmetric excitation ($l_1 = l_2$, Fig. 1(d)) then may be expressed as [5]

$$\Gamma_N \simeq \Gamma_{ss}\sum_{\nu=1}^{N}\exp\{-2l_1(\nu - 1) \cdot [(\alpha_H + \alpha_L) + j(\beta_H + \beta_L)]\} \tag{6}$$

where α_L and β_L are the attenuation and phase constants of the low-photoconductivity sections. Since multiple reflections are neglected, an error of $\leqq 4\%$ is introduced as long as $|\Gamma_N| \leqq 40\%$ [14]. Referring to the low-excitation condition again, β_H and β_L are obtained from [5]

$$\beta_H \simeq \beta_L \simeq \beta_l = (\omega^2\mu_0\mu_r\epsilon_0\epsilon_{re})^{1/2} \tag{7}$$

where β_l is the phase constant of a lossless CPW and μ_0 and μ_r are the free-space and relative permeabilities, respectively. α_H and α_L can be approximately calculated from [5]

$$\alpha_{H,L} \simeq \alpha_0 + \Delta\vartheta_{H,L}\beta_l/2 \tag{8}$$

where α_0 is the frequency-dependent attenuation constant of the dark silicon CPW used [9].

Further, the relationship between center frequency f_c and specific grating length l_1 is given by

$$f_c = 1/4l_1(\mu_0\mu_r\epsilon_0\epsilon_{re})^{1/2} \tag{9}$$

assuming $\Delta\vartheta_{H,L} \ll 1$ and $N \gg 1$ [5], [9]. Finally, this improved DBR analysis can be easily checked via the limiting condition of negligible longitudinal carrier diffusion according to $l_1/L_a \to \infty$, yielding $\Delta\sigma_H = \Delta\sigma_e$ and $\Delta\sigma_L = 0$ from (3). These are the constant-level step heights of the simplified stepped-impedance model used formerly [8], [9].

The spectral dependence of Γ_N is manifested by the wavelength-dependent quantities $\Delta\vartheta_e(\lambda)$ and $\Delta\sigma_e(\lambda)$, respectively, which govern $Z_{H,L}(\lambda)$ and $\alpha_{H,L}(\lambda)$ in accordance with (1) and (8). Hence, it is quite consistent to analyze $\Delta\vartheta_e$ in detail (Section III) with explicit regard to all the wavelength-dependent quantities being incorporated into $\Delta\vartheta_e$. As an anticipatory result from the following analysis, it is seen that the spectral response of $\Delta\vartheta_e$ is caused by the spectral dependence of the inherent DBR sensitivity κ (Section III) which dominates the spectral dependence of $\Gamma_N(\lambda)$ via $Z_{H,L}(\lambda)$. The influence of $\kappa(\lambda)$ on $\Gamma_N(\lambda)$ via $\alpha_{H,L}(\lambda)$ is found to be of secondary importance.

III. Definition and Spectral Dependence of DBR Sensitivity

Referring to detailed investigations on the transverse diffusion mechanisms and surface recombination processes in a photoexcited semiconductor CPW [4], [11], [15], $\Delta\sigma_e$ can be expressed as

$$\Delta\sigma_e = (q/hc)(\mu_n + \mu_p)(1 - R)S_\lambda\lambda_p\alpha_r\tau F_1F_2p \tag{10}$$

where q is the electronic charge, h is Planck's constant, c is the velocity of light in free space, μ_r and μ_p are the mobilities of electrons and holes, and S_λ is the relative spectral response of the semiconductor material[1] exhibiting a peak response at the optical wavelength λ_p (Fig. 3(a)). R is the surface reflectivity

[1] From manufacturer's specification sheet (Siemens AG, Munich).

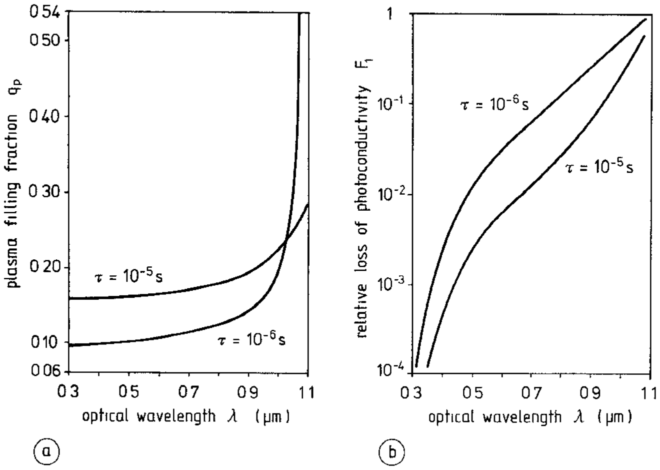

Fig. 4. (a) Plasma filling fraction q_p and (b) diffusion-controlled relative loss of photoconductivity F_1 of the prototype silicon CPW as a function of optical wavelength λ with charge carrier lifetime τ as parameter; ($S = 710$ µm, $W = 460$ µm, $H = 500$ µm, $v_s = 2000$ cm/s, $T = 300$K).

at λ_p, α_r is the radiation absorption coefficient (Fig. 3(b)) [16], τ is the carrier lifetime, and p is the controlling irradiance. F_1 covers the relative loss of photoconductivity through carrier diffusion into the direction of surface normal, which is due to absorption and surface recombination, according to [11], [15]

$$F_1 = (1 + \alpha_r L_a)^{-1}\left[\frac{1}{\alpha_r L_a}\left(\frac{\alpha_r L_a^2 + v_s\tau}{L_a + v_s\tau}\right)\right]^{-\alpha_r L_a/(1-\alpha_r L_a)} \quad (11)$$

where v_s is the surface recombination velocity, and L_a is the ambipolar diffusion length given by

$$L_a = [(2\mu_n\mu_p\tau kT/q)(\mu_n + \mu_p)^{-1}]^{1/2} \quad (12)$$

with the absolute temperature T and Boltzmann's constant k.

The relative loss of photoconductivity through lateral carrier diffusion into the dark substrate regions (which are shaded by the CPW electrodes) is considered by F_2, according to [4], [15]

$$F_2 \simeq \frac{(W/4L_a)(1-\zeta^2)^{1/2}}{Arth[(1-\zeta)/(1+\zeta)]^{1/2}} \quad (13a)$$

with

$$\zeta = \exp(-W/2L_a) \quad (13b)$$

and slot width W of CPW (Fig. 2(a)). By substituting (10) into (2), $\Delta\vartheta_e$ can be rewritten as

$$\Delta\vartheta_e = \left[\frac{q(\mu_n + \mu_p)(1-R)q_\epsilon\lambda_p\tau F_2}{2\pi hc\epsilon_0\epsilon_{re}} S_\lambda \alpha_r q_p F_1\right]\frac{p}{f} \quad (14a)$$

where the term in square brackets denotes the inherent DBR sensitivity κ of an optoelectronic CPW grating [11]. For practical reasons, (14a) may be rewritten in the form

$$\Delta\vartheta_e(\lambda) = \kappa(\lambda)p/f = \kappa_n(\lambda)(p/mWcm^{-2})/(f/GHz) \quad (14b)$$

with the normalized (dimensionless) DBR sensitivity $\kappa_n = \kappa \times 10^{-12}VAs$ cm^{-2}.

Referring to (14a), the spectral dependence of κ (or κ_n) is determined by the product of $S_\lambda(\lambda)$ and $\alpha_r(\lambda)$ (Fig. 3), $q_p(\lambda)$, and $F_1(\lambda)$. The plasma filling fraction q_p can be evaluated from a quasi-static analysis of photoinduced

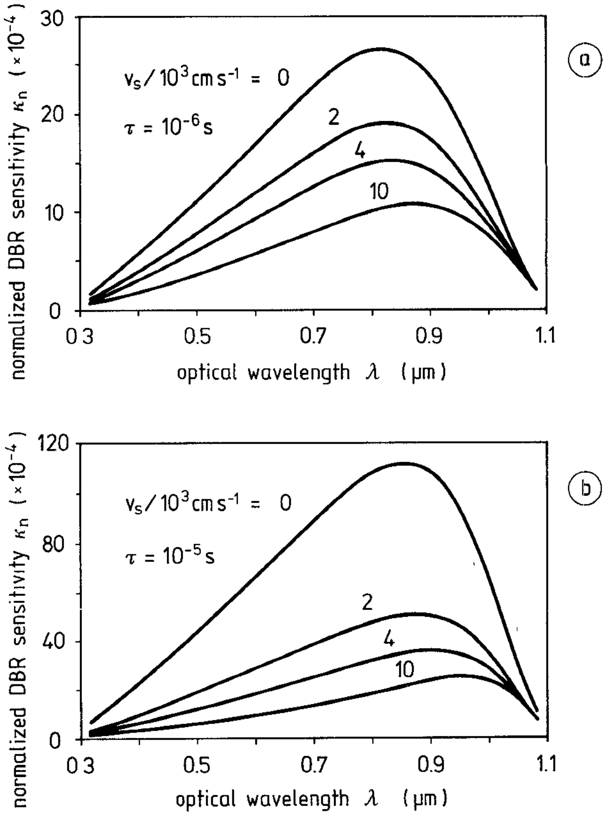

Fig. 5. Calculated spectral dependence of normalized DBR sensitivity κ_n of the prototype silicon CPW with surface recombination velocity v_s as parameter in the case of (a) $\tau = 10^{-6}s$ and (b) $\tau = 10^{-5}s$; ($S = 710$ µm, $W = 460$ µm, $H = 500$ µm, $T = 300$K).

wave attenuation in a semiconductor CPW, using a conformal mapping technique [4]. As a result, q_p appears as a function of normalized plasma penetration depth δ where $q_p(\delta)$ has to be evaluated numerically. δ itself, however, can be expressed as [4], [15]

$$\delta = \frac{2}{S\alpha_r}\left[\frac{L_a(1+\alpha_r L_a) + v_s\tau}{L_a + v_s\tau}\right] \cdot \left[\frac{1}{\alpha_r L_a}\left(\frac{\alpha_r L_a^2 + v_s\tau}{L_a + v_s\tau}\right)\right]^{\alpha_r L_a/(1-\alpha_r L_a)} \quad (15)$$

where S is the strip width of CPW (Fig. 2(a)). It is seen that δ is a wavelength-dependent quantity via $\alpha_r(\lambda)$, resulting in $q_p = q_p(\lambda)$. For example, Fig. 4(a) shows q_p of the prototype silicon CPW ($S = 710$ µm, $W = 460$ µm, substrate thickness $H = 500$ µm, $Z_l = 50\,\Omega$, $v_s = 2000$ cm/s [9]) as a function of λ with τ as parameter. Finally, the spectral dependence of $F_1(\lambda)$, also imposed by $\alpha_r(\lambda)$, can be easily obtained from (11) (Fig. 4(b)). Referring to (14) again, the total spectral dependence of κ_n can be evaluated now. As a result, Fig. 5 shows $\kappa_n(\lambda)$ of the aforementioned silicon CPW with v_s as parameter for $\tau_a = 10^{-6}s$ and $\tau_b = 10^{-5}s$, substituting $(\mu_n + \mu_p) = 2100$ cm^2/Vs, $R = 0.30$, $q_\epsilon = 0.50$, $\epsilon_{re} = 6.432$ [9], $\lambda_p = 860$ nm, $F_2(\tau_a) = 0.8760$, and $F_2(\tau_b) = 0.6783$.

IV. Results and Concluding Remarks

As a final step of analysis, the spectral dependence of light-induced microwave reflection coefficient (at arbitrary signal

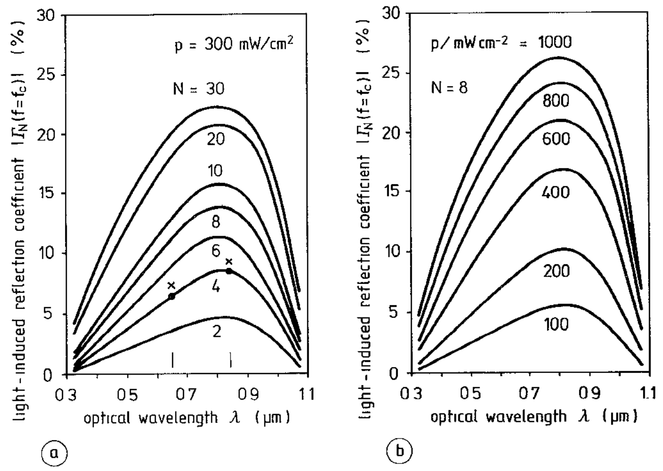

Fig. 6. Calculated spectral dependence of light-induced major-lobe peak reflection coefficient $|\Gamma_N(f = f_c)|$ from the prototype silicon CPW with (a) number of grating elements N as parameter for $p = 300$ mW/cm^2, and with (b) incident CW irradiance p as parameter for $N = 8$; ($l_1 = l_2 = 0.27$ cm, $f = f_c = 11$ GHz, $\tau = 10^{-6}s$, $v_s = 2000$ cm/s, $T = 300$K). Experimental results ($\times$) and their corresponding calculated values ($\bullet$) are recorded, as well.

frequency f, in general) can be easily calculated from (6), bearing in mind that Γ_{st} as well as $\alpha_{H,L}$ are conditioned by $\kappa_n(\lambda)$ via $\Delta\vartheta_{H,L}(\kappa_n)$. In most cases of interest, the goal of optimization procedure is to achieve maximum reflectance at the center frequency. Hence, it is quite consistent to evaluate the spectral dependence of light-induced major-lobe peak reflection coefficient $|\Gamma_N(f = f_c)|$. Corresponding results from the prototype silicon CPW are presented in Fig. 6 with N and p as parameters. It is seen that the spectral performance of peak reflection coefficient is very similar to that of DBR sensitivity (Fig. 5(a), $v_s = 2000$ cm/s), both exhibiting maximum response at about 825 nm, which is the optimum wavelength of excitation in this case.

Referring to the assumption $\Delta\vartheta_{H,L} \ll 1$ again, from (4) one obtains $|\Gamma_{st}(\lambda)| \propto \Delta\vartheta_{H,L}(\lambda)$, and hence $|\Gamma_{st}(\lambda)| \propto \kappa_n(\lambda)$. With special regard to this latter relation, a detailed discussion of (6) reveals that the overall spectral response is clearly dominated by $\kappa_n(\lambda)$, while the influence via $\alpha_{H,L}(\lambda)$ is of little significance. This second-order dependence causes only a slight downward shift of optimum wavelength by some few nanometers with an increase in N or p, respectively (Fig. 6). Thus, the optimization of DBR microwave performance with respect to the excitation wavelength may be successfully accomplished via $\kappa_n(\lambda)$ rather than $\Gamma_N(\lambda)$, so reducing numerical effort.

Moreover, it is seen that the optimum wavelength appears quite close to λ_p of the relative photosensitivity (Fig. 3(a)). This is not necessarily the case, and is due here to the given constellation of the CPW dimensions, i.e., H, S, and W. Referring to similar investigations with GaAs, InP, and CdS, the aforementioned cognitions have been found to be independent of semiconductor material, thus rising the theory presented here to apply generally. As the spectral dependence of DBR characteristics and, in consequence, the optimum wavelength of excitation are governed by transverse carrier diffusion (and, thus, are sensitive to the CPW dimensions), H, S, and W can be also considered as quantities that may be engineered to optimize device performance. A corresponding overall optimization of a full-silicon CPW grating, involving τ, v_s, λ, H, S, W, N, and p along with $l_1 \neq l_2$, is currently in progress.

The overall accuracy of the calculated results may be estimated from the individual accuracies of the conformal mapping technique (CMT) on the one hand and the improved stepped-impedance model (ISIM) on the other. The validity of the CMT used implies limited ranges of values of the basic microwave and optoelectronic parameters, which has been extensively discussed in prior publications [4], [5]. From this, a CTM accuracy of $\leq 28\%$ is obtained for the chosen parameters according to Fig. 6 along with an arbitrary v_s, $\tau \leq 10^{-4}s$, and $f_c = 1$–30 GHz. The ISIM accuracy can be evaluated from a worst-case error estimation of $\Gamma_N(f = f_c)$ as a function of p, N, and f_c, which has been reported recently [17]. Herein, the worst-case condition is defined as $l_1/L_a = 4$, which means very strong carrier diffusion into the direction of wave propagation and, hence, results in a very low contrast ratio $\Delta\sigma_H/\Delta\sigma_L = 6.4$. In this (worst) case, the distribution of induced photoconductivity $\Delta\sigma(z)$ is quite similar to a sinusoidal profile which, of course, has no importance with respect to any application, but allows the error estimation to be performed through strongly reduced numerical effort. As a result, the maximum error of the major-lobe peak reflection coefficient amounts to 37% in magnitude and 11° in phase [17]. However, when assuming $\tau \leq 10^{-4}s$ again along with $l_1/L_a \geq 20$ and $\Delta\sigma_H/\Delta\sigma_L \geq 2.2 \times 10^3$ for successful applications, the specific ISIM error becomes negligible [17]. Thus, the overall accuracy may be estimated as $\leq 28\%$ for $p \leq 10^3$ mWcm^{-2}, $N \geq 2$, and $f_c = 1$–30 GHz.

Concerning the experimental verification of $\kappa_n(\lambda, v_s)$ and $|\Gamma_N(\lambda, v_s, N)|$, it is well understood that a change of λ through the full range from 0.3 μm up to 1.1 μm or a variation of v_s from 0 to 10^4 cm/s, or an increase in N from 2 through 20 is not easy to accomplish in practice.

Until now, some experiments with two different excitation wavelengths have been performed. First, an 11-GHz four-element grating structure ($N = 4$) was induced by 840 nm 110 mWcm^{-2} LED-excitation of a full-substrate silicon CPW with $\tau = 10^{-6}s$ and $v_s = 2000$ cm/s [9], using a configuration quite similar to that shown in Fig. 2. Through a suitable change of the illumination pattern, an eight-element grating ($N = 8$) was obtained resulting in a changeover of center frequency to 22 GHz. Fig. 7 shows the measured and calculated reflection spectra, where the illumination pattern coefficient $n = 0$ indicates symmetric excitation with $l_1 = l_2$ [9]. It is seen that the discrepancy between theory and experiment is relatively small and, particularly for the major-lobe peak reflection coefficients, amounts to less than 5% at the given parameter constellation. In a recent experiment, the four-element grating again was induced by $p = 300$ mWcm^{-2} at $\lambda = 840$ nm, resulting in $|\Gamma_4(11\,\text{GHz})| = 9.2\%$. The corresponding calculated reflection coefficient is 8.4%. Both values are recorded in Fig. 6(a).

Second, another full-substrate silicon CPW with unprotected, naturally oxidized surfaces (with $v_s = 10^4$ cm/s and $\tau = 10^{-6}s$) was excited by a krypton ion laser radiating at 647

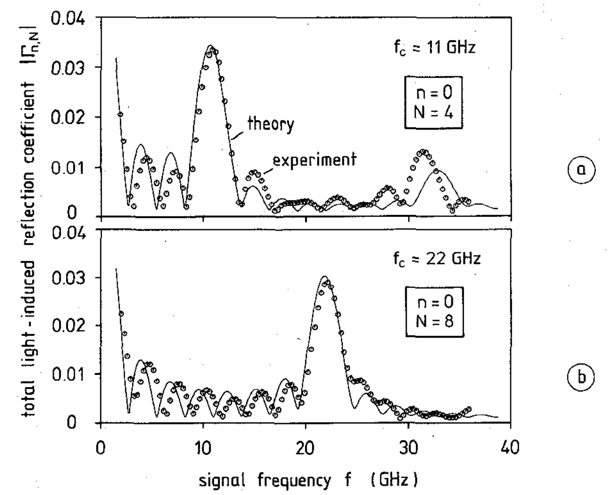

Fig. 7. Measured and calculated reflection spectra of a silicon coplanar waveguide LED-induced DBR microwave filter with optically controlled change of center frequency from (a) 11 GHz to (b) 22 GHz [9]. The optical excitation was $p = 110$ mWcm^{-2} at $\lambda = 840$ nm with $\tau = 10^{-6} s$ and $v_s = 2000$ cm/s. ($n = 0$ means $l_1 = l_2$).

nm and supplying an irradiance of $p = 440$ mWcm^{-2} from the fiber bundle output [11]. The induced grating structure was characterized by $N = 4$ and $f_c = 11$ GHz. The measured major-lobe peak reflection coefficient was 3.7%; this theory yields 4.4%. Likewise, the aforementioned silicon substrate CPW with etched surfaces (with $v_s = 2000$ cm/s and $\tau = 10^{-6} s$) was excited by $p = 300$ mWcm^{-2}. A major-lobe peak reflection coefficient of 7.4% at 11 GHz could be measured, whereas this theory yields 6.5%. Both values are recorded in Fig. 6(a), as well.

Finally, as a more futuristic idea, the disadvantage of substantially reduced DBR efficiency through optically induced losses could be overcome in replacing the full-semiconductor substrate by a conditional artificial dielectric (CAD) [18]. This is a composite of small semiconductor crystallites embedded in a polymeric host material. On illumination, the optically induced electric and magnetic dipoles in each obstacle increase the effective dielectric constant rather than the photoconductivity. Once matured, this approach could significantly improve the spectral and microwave performances of optoelectronic waveguide gratings.

Acknowledgment

The author gratefully acknowledges the constructive criticism of the reviewers.

References

[1] T. Itoh, "Application of gratings in a dielectric waveguide for leaky-wave antennas and band-reject filters," *IEEE Trans. Microwave Theory Tech.*, vol. MTT-25, pp. 1134–1138, 1977.

[2] T. Itoh and F. J. Hsu, "Distributed Bragg reflector Gunn oscillators for dielectric millimeter-wave integrated circuits," *IEEE Trans. Microwave Theory Tech.*, vol. MTT-27, pp. 514–518, 1979.

[3] B. S. Song and T. Itoh, "Distributed Bragg reflection dielectric waveguide oscillators," *IEEE Trans. Microwave Theory Tech.*, vol. MTT-27, pp. 1019–1022, 1979.

[4] W. Platte and B. Sauerer, "Optically CW-induced losses in semiconductor coplanar waveguides," *IEEE Trans. Microwave Theory Tech.*, vol. 37, pp. 139–149, 1989.

[5] W. Platte, "Periodic-structure photoexcitation of a silicon coplanar waveguide for selective optoelectronic microwave control," *IEEE Trans. Microwave Theory Tech.*, vol. 38, pp. 638–646, 1990.

[6] W. Platte, "Influence of charge carrier diffusion on the microwave performance of fiber-optically generated DBR filter structures," Arch. Elek. Übertragung., vol. 44, pp. 282–290, 1990 (in German).

[7] W. Platte, "Improved analysis of optoelectronic waveguide gratings operated at microwave and millimeter wave frequencies," Arch. Elek. Übertragung., vol. 47, pp. 30–37, 1993 (in German).

[8] W. Platte, "Optical control of microwaves by LED-induced DBR structures in silicon coplanar waveguides," *Electron. Lett.*, vol. 25, pp. 177–179, 1989.

[9] W. Platte, "LED-induced distributed Bragg reflection microwave filter with fiber-optically controlled change of center frequency via photoconductivity gratings," *IEEE Trans. Microwave Theory Tech.*, vol. 39, pp. 359–363, 1991.

[10] W. Platte, "Fiber-optically induced DBR microwave filter structures with optimized reflection and selectivity characteristics," Arch. Elek. Übertragung., vol. 44, pp. 291–296, 1990 (in German).

[11] W. Platte, "Effect of surface recombination on microwave performance of laser-induced DBR gratings in silicon coplanar waveguides," in *Proc. Inst. Elec. Eng., pt. J.*, 1992, vol. 139, pp. 399–401.

[12] K. C. Gupta, R. Garg, and I. J. Bahl, *Microstrip Lines and Slotlines.* Norwood, MA: Artech House, 1979.

[13] W. Platte, "Longitudinal conductivity profile in periodically photoexcited semiconductor transmission lines," in *Proc. Inst. Elec. Eng., pt. J.*, 1989, vol. 136, pp. 108–110.

[14] R. E. Collin, *Foundations for Microwave Engineering.* New York: McGraw-Hill, 1966, pp. 224–254.

[15] W. Platte, "Effective photoconductivity and plasma depth in optically quasi-CW controlled microwave switching devices," in *Proc. Inst. Elec. Eng., pt. J.*, 1988, vol. 135, pp. 251–254.

[16] W. C. Dash and R. Newman, "Intrinsic optical absorption in single-crystal germanium and silicon at 77K and 300K," *Phys. Rev.*, 1955, vol. 99, pp. 1151–1155.

[17] W. Platte, "Worst-case error estimation of the diffusion-dependent stepped-impedance model of optoelectronic waveguide gratings," *Archiv für Elektrotechnik,* vol. 76, pp. 249–256, 1993 (in German).

[18] H. Grebel and P. Chen, "Artificial dielectric polymeric waveguides: semiconductor-embedded films," *Optics Lett.*, vol. 15, pp. 667–669, 1990.

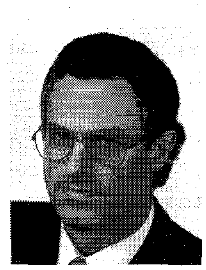

Walter Platte was born in Remscheid-Lennep, Germany, on January 24, 1943. He received the Dipl.-Ing. degree in electrical engineering from the Technical University of Aachen, Aachen, Germany, in 1968 and the Dr.-Ing. degree in electrical engineering and the Habilitation degree ("venia legendi") from the University of Erlangen-Nuernberg, Erlangen, Germany, in 1975 and 1986, respectively.

From 1968 to 1969, he worked at AEG-Telefunken, Ulm, Germany, on Ku-band radar instrumentation and measurement, in particular Doppler radar moving target simulators. From 1969 to 1990, he was with the Department of High-Frequency Techniques, University of Erlangen-Nuernberg, where he worked as a research assistant, senior assistant, and adjunct staff member (Privat-Dozent) engaged in research on laser-controlled MIC and millimeter wave components, optoelectronics, and optical communications.

Since October 1990, he has been a professor of electrical engineering and Head of the Department of High-Frequency and Optoelectronic Engineering, University of the Federal Armed Forces, Hamburg, Germany. His research interests include optical techniques for microwave and millimeter wave applications, lightwave technology, fiber sensors, and electromagnetic compatibility.

Prof. Platte is a member of the Verband Deutscher Elektrotechniker (VDE/NTG). He was awarded the Annual Prize of the Nachrichtentechnische Gesellschaft (NTG) in 1977 and the Finkelnburg Habilitation Prize of the University of Erlangen-Nuernberg in 1987.